

# Search for the Blazhko effect in field RR Lyrae stars using LINEAR and ZTF light curves

Ema Donev<sup>1</sup> and Željko Ivezić<sup>2</sup>

<sup>1</sup> XV. Gymnasium (MIOC), Jordanovac 8, 10000, Zagreb, Croatia, e-mail: emadonev@icloud.com

<sup>2</sup> Department of Astronomy and the DiRAC Institute, University of Washington, 3910 15th Avenue NE, Seattle, WA, USA e-mail: ivezic@uw.edu

October 2024

## ABSTRACT

We analyzed the incidence and properties of RR Lyrae stars that show evidence for amplitude and phase modulation (the so-called Blazhko Effect) in a sample of  $\sim 3,000$  stars with LINEAR and ZTF light curve data. A preliminary subsample of about  $\sim 240$  stars was algorithmically pre-selected using various data quality and light curve statistics, and then 139 stars were confirmed visually as displaying the Blazhko effect. This sample places a lower limit of 5% for the incidence of the Blazhko Effect in field RR Lyrae stars. Although close to 8,000 Blazhko stars were discovered or confirmed in the Galactic bulge and LMC/SMC by the OGLE-III survey, only about 200 stars have been reported in all field RR Lyrae stars studies to date; the sample presented here nearly doubles the number of field RR Lyrae stars displaying the Blazhko effect. With time-resolved photometry expected from LSST, a similar analysis will be performed for RR Lyrae stars in the southern sky and we anticipate a higher fraction of discovered Blazhko stars due to better sampling and superior photometric quality.

**Key words.** Variable stars — RR Lyrae stars — Blazhko Effect

## 1. Introduction

RR Lyrae stars are pulsating variable stars with periods in the range of 3–30 hours and large amplitudes that increase towards blue optical bands (e.g., in the SDSS  $g$  band from 0.2 mag to 1.5 mag; Sesar et al. 2010). For comprehensive reviews of RR Lyrae stars, we refer the reader to Smith (1995) and Catelan (2009).

RR Lyrae stars often exhibit amplitude and phase modulation, or the so-called Blazhko effect<sup>1</sup> (hereafter, “Blazhko stars”). For examples of well-sampled observed light curves showing the Blazhko effect, see, e.g., Kepler data shown in Figures 1 and 2 from Benkő et al. (2010). The Blazhko effect has been known for a long time (Blažko 1907), but its detailed observational properties and theoretical explanation of its causes remain elusive (Kolenberg 2008; Kovács 2009; Szabó 2014). Various proposed models for the Blazhko effect, and principal reasons why they fail to explain observations, are summarized in Kovacs (2016).

A part of the reason for the incomplete observational description of the Blazhko effect is difficulties in discovering a large number of Blazhko stars due to temporal baselines that are too short and insufficient number of observations per object (Kovacs 2016; Hernitschek & Stassun 2022). With the advent of modern sky surveys, several studies reported large increases in the number of known Blazhko stars, starting with a sample of about 700 Blazhko stars discovered by the MACHO survey towards the LMC (Alcock et al. 2003) and about 500 Blazhko stars discovered by the OGLE-II survey towards the Galactic bulge (Mizerski 2003). Most recently, about 4,000 Blazhko stars were discovered in the LMC and SMC (Soszyński et al. 2009, 2010),

and an additional  $\sim 3,500$  stars were discovered in the Galactic bulge (Soszyński et al. 2011; Prudil & Skarka 2017), both by the OGLE-III survey. Nevertheless, discovering the Blazhko effect in field RR Lyrae stars that are spread over the entire sky remains a much harder problem: only about 200 Blazhko stars in total from all the studies of field RR Lyrae stars have been reported so far (see Table 1 in Kovacs 2016).

Here, we report the results of a search for the Blazhko effect in a sample of  $\sim 3,000$  field RR Lyrae stars with LINEAR and ZTF light curve data. A preliminary subsample of about  $\sim 240$  stars was selected using various light curve statistics, and then  $\sim 140$  stars were confirmed visually as displaying the Blazhko effect. This new sample greatly increases the number of known field RR Lyrae stars that exhibit the Blazhko effect. In §2 and §3 we describe our datasets and analysis methodology, and in §4 we present our analysis results. Our main results are summarized and discussed in §5.

## 2. Data Description and Period Estimation

Analysis of field RR Lyrae stars requires a sensitive time-domain photometric survey over a large sky area. For our starting sample, we used  $\sim 3,000$  field RR Lyrae stars with light curves obtained by the LINEAR asteroid survey. In order to study long-term changes in light curves, we also utilized light curves obtained by the ZTF survey which monitored the sky  $\sim 15$  years after LINEAR. The combination of LINEAR and ZTF provided a unique opportunity to systematically search for the Blazhko effect in a large number of field RR Lyrae stars.

<sup>1</sup> The Blazhko effect was discovered by Lidiya Petrovna Tseraskaya and first reported by Sergey Blazhko.

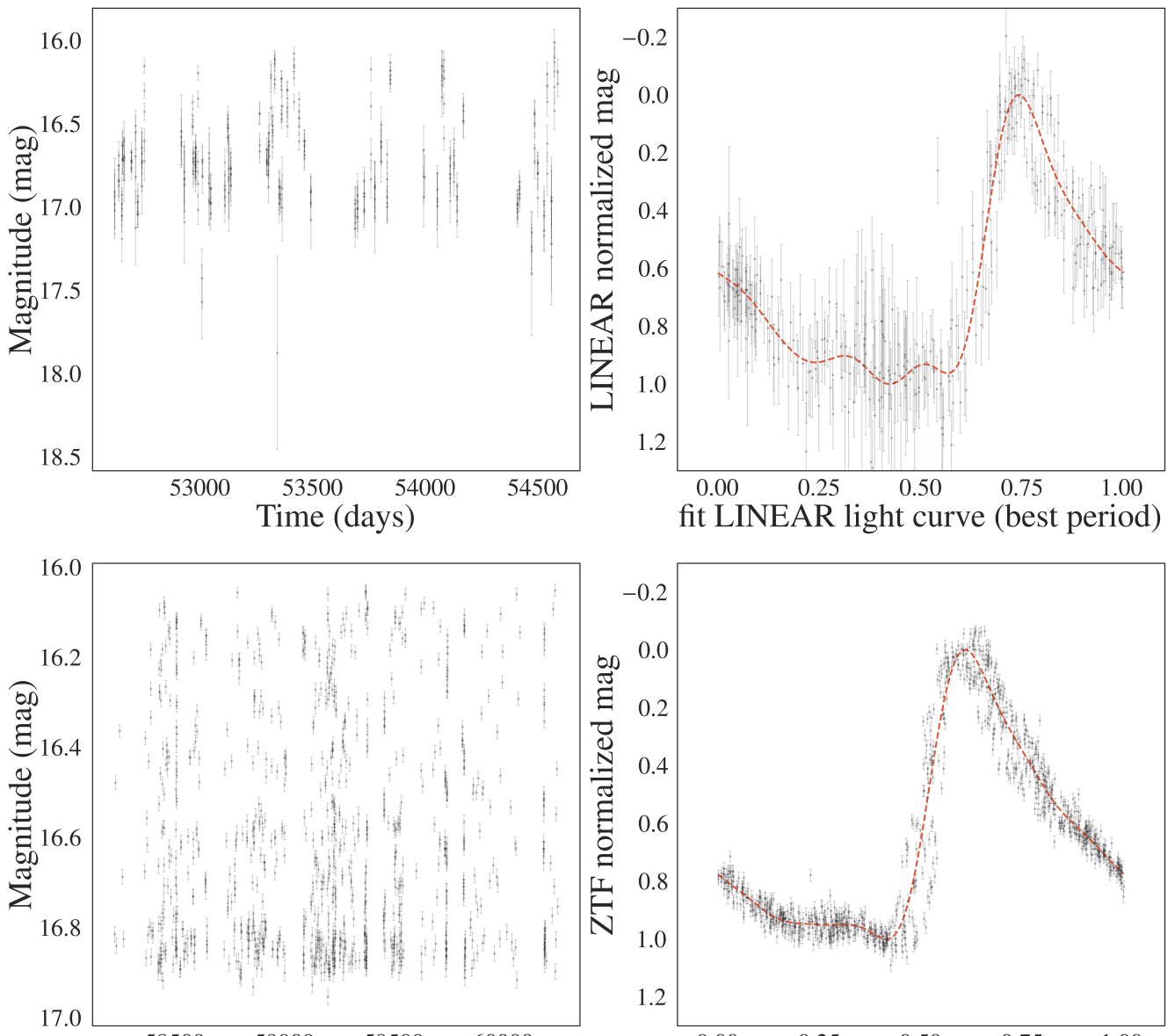


**Fig. 1.** An example of a Blazhko star (LINEARid = 1212611) with LINEAR (top row) and ZTF (bottom row) light curves (left panels, data points with “error bars”), phased light curves from 0 to the 0–1 range (right panels, data points with “error bars”), the best-fit model shown by dashed lines. The best-fit period is determined for each dataset separately using 3 Fourier terms. The models shown in the right panels are evaluated with 6 Fourier terms.

58 We first describe each dataset in more detail, and then introduce our analysis methods. All our analysis code, written in  
 59 Python, is available on GitHub<sup>2</sup>.  
 60

### 61 2.1. LINEAR Dataset

62 The properties of the LINEAR asteroid survey and its photometric re-calibration based on SDSS data are discussed in Sesar  
 63 et al. (2011). Briefly, the LINEAR survey covered about 10,000  
 64 deg<sup>2</sup> of the northern sky in white light (no filters were used, see  
 65 Figure 1 in Sesar et al. 2011), with photometric errors ranging  
 66 from ~0.03 mag at an equivalent SDSS magnitude of  $r = 15$  to  
 67 0.20 mag at  $r \sim 18$ . Light curves used in this work include, on  
 68 average, 270 data points collected between December 2002 and  
 69 September 2008.  
 70

A sample of 7,010 periodic variable stars with  $r < 17$  discovered in LINEAR data were robustly classified by Palaversa et al. (2013), including about ~3,000 field RR Lyrae stars of both ab and c type, detected to distances of about 30 kpc (Sesar et al. 2013). The sample used in this work contains 2196 ab-type and 745 c-type RR Lyrae, selected using classification labels and the  $gi$  color index from Palaversa et al. (2013). The LINEAR light curves, augmented with IDs, equatorial coordinates, and other data, were accessed using the astroML Python module<sup>3</sup> (VanderPlas et al. 2012).

### 71 2.2. ZTF Dataset

72 The Zwicky Transient Factory (ZTF) is an optical time-domain  
 73 survey that uses the Palomar 48-inch Schmidt telescope and a  
 74

<sup>2</sup> [https://github.com/emadonev/var\\_stars](https://github.com/emadonev/var_stars)

<sup>3</sup> For an example of light curves, see [https://www.astroml.org/book\\_figures/chapter10/fig\\_LINEAR\\_LS.html](https://www.astroml.org/book_figures/chapter10/fig_LINEAR_LS.html)

camera with 47 deg<sup>2</sup> field of view (Bellm et al. 2019). The dataset analyzed here was obtained with SDSS-like *g*, *r*, and *i* band filters. Light curves for objects in common with the LINEAR RR Lyrae sample typically have smaller random photometric errors than LINEAR light curves because ZTF data are deeper (compared to LINEAR, ZTF data have about 2-3 magnitudes fainter 5 $\sigma$  depth). ZTF data used in this work were collected between February 2018 and December 2023, on average about 15 years after obtaining LINEAR data.

The ZTF dataset for this project was created by selecting ZTF IDs with matching equatorial coordinates to a corresponding LINEAR ID of an RR Lyrae star. This process used the *ztfquery* function, which searched the coordinates in the ZTF database within 3 arcsec from the LINEAR position. The resulting sample consisted of 2857 RR Lyrae stars with both LINEAR and ZTF data. The fractions of RRab and RRc type RR Lyrae in this sample, 71% RRab and 29% RRc type, are consistent with results from other surveys (e.g., Sesar et al. 2010).

### 2.3. Period Estimation

The first step of our analysis is estimating best-fit periods, separately for LINEAR and ZTF datasets. We used the Lomb-Scargle method (Vanderplas 2015) as implemented in *astropy* (Astropy Collaboration et al. 2018). The period estimation used 3 Fourier components and a two-step process: an initial best-fit frequency was determined using the *autopower* frequency grid option and then the power spectrum was recomputed around the initial frequency using an order of magnitude smaller frequency step. In case of ZTF, we estimated period separately for each available passband and adopted their mean value. Once the best-fit period was determined, a best-fit model for the phased light curve was computed using 6 Fourier components. Fig 1 shows an example of a star with LINEAR and ZTF light curves, phased light curves, and their best-fit models.

We found excellent agreement between the best-fit periods estimated separately from LINEAR and ZTF light curves. The median of their ratio is unity within  $2 \times 10^{-6}$  and the robust standard deviation of their ratio is  $2 \times 10^{-5}$ . With a median sample period of 0.56 days, the implied scatter of period difference is about 1.0 sec.

Given on average about 15 years between LINEAR and ZTF data sets, and a typical period of 0.56 days, this time difference corresponds to about 10,000 oscillations. With a fractional period uncertainty of  $2 \times 10^{-5}$ , LINEAR data can predict the phase of ZTF light curve with an uncertainty of 0.2. Therefore, for a robust detection of light curve phase modulation, each data set must be analyzed separately. On the other hand, amplitude modulation can be detected on time scales as long as 15 years, as discussed in the following section.

## 3. Analysis Methodology: Searching for the Blazhko Effect

Given the two sets of light curves from LINEAR and ZTF, we searched for amplitude and phase modulation, either during the 5-6 years of data taking by each survey, or during the average span of 15 years between the two surveys. Starting with a sample of 2857 RR Lyrae stars, we pre-selected a smaller sample that was inspected visually (see below for details). We also required at least 250 LINEAR data points and 40 ZTF data points (per band) in analyzed light curves. We used two pre-selection methods that are sensitive to different types of light curve mod-

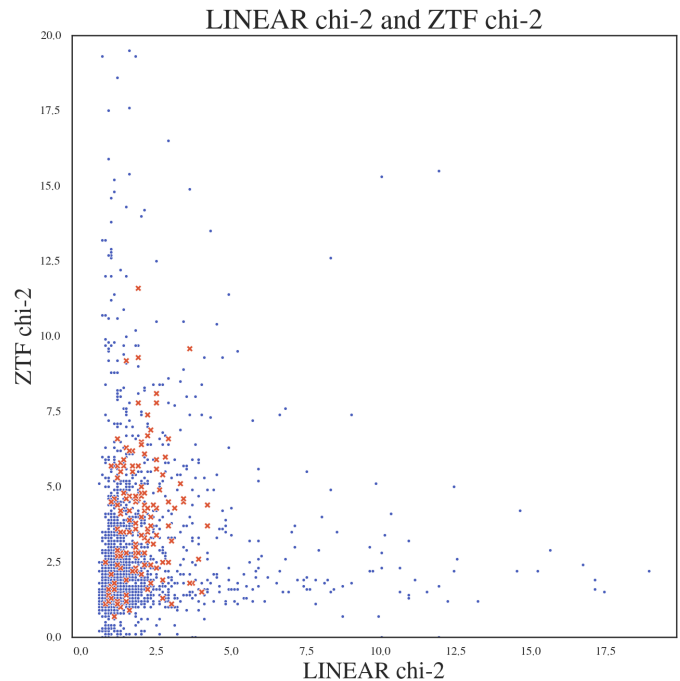


**Fig. 2.** A selection diagram constructed with the two sets of robust  $\chi^2_{dof}$  values, for LINEAR and ZTF data sets, where blue symbols represents all RR Lyrae stars and the red symbols are the final sample of Blazhko stars. The horizontal and vertical dashed lines mark Blazhko candidate selection boundaries (see text).

ulation: direct light curve analysis and periodogram analysis, as follows.

### 3.1. Direct Light Curve Analysis

Given statistically correct period, amplitude and light curve shape estimates, as well as data being consistent with reported (presumably Gaussian) uncertainty estimates, the  $\chi^2$  per degree of freedom gives a quantitative assessment of the "goodness of fit",

$$\chi^2_{dof} = \frac{1}{N_{dof}} \sum \frac{(d_i - m_i)^2}{\sigma_i^2}. \quad (1)$$

Here,  $d_i$  are measured light curve data values at times  $t_i$ , and with associated uncertainties  $\sigma_i$ ,  $m_i$  are best-fit models at times  $t_i$ , and  $N_{dof}$  is the number of degrees of freedom, essentially the number of data points. In the absence of any light curve modulation, the expected value of  $\chi^2_{dof}$  is unity, with a standard deviation of  $\sqrt{2/N_{dof}}$ . If  $\chi^2_{dof} - 1$  is many times larger than  $\sqrt{2/N_{dof}}$ , it is unlikely that data  $d_i$  were generated by the assumed (unchanging) model  $m_i$ . Of course,  $\chi^2_{dof}$  can also be large due to underestimated measurement uncertainties  $\sigma_i$ , or to occasional non-Gaussian measurement error (the so-called outliers).

Therefore, to search for signatures of the Blazhko effect, manifested through statistically unlikely large values of  $\chi^2_{dof}$ , we computed  $\chi^2_{dof}$  separately for LINEAR and ZTF data (see Figure 2). Using the two sets of  $\chi^2_{dof}$  values, we algorithmically pre-selected a sample of candidate Blazhko stars for further visual analysis of their light curves. The visual analysis is needed to confirm the expected Blazhko behavior in observed light curves, as well as to identify cases of data problems, such as photometric outliers.

# Analysis of blazhko star metrics for RR Lyrae

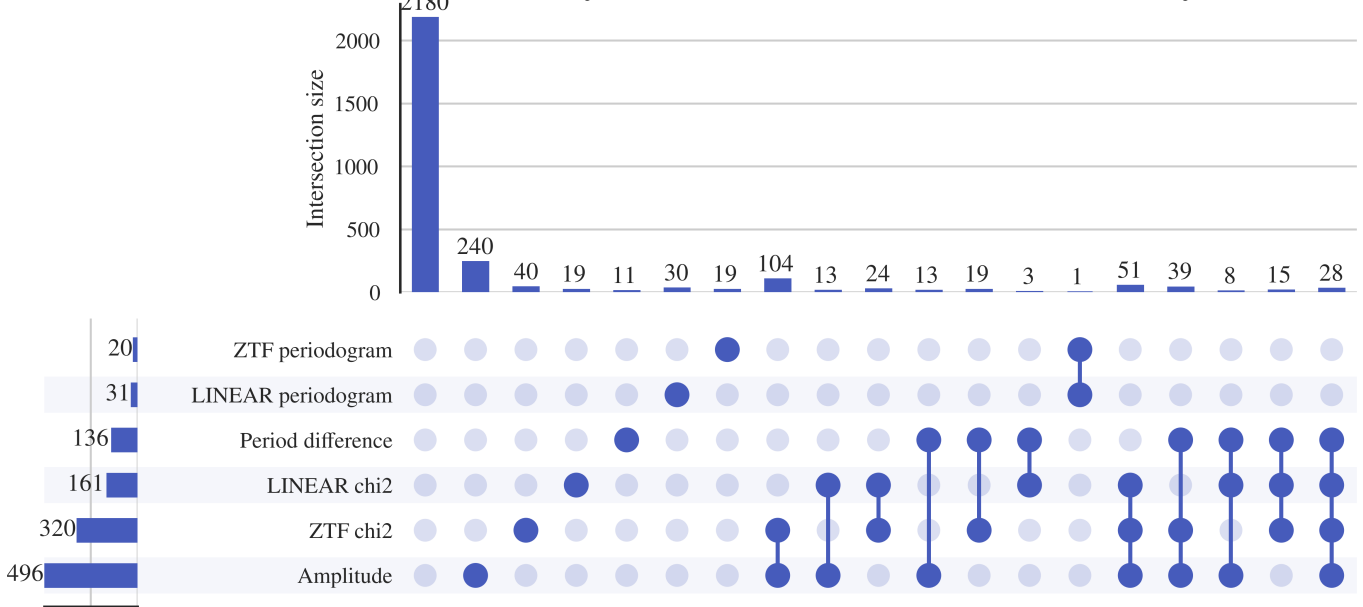


**Fig. 3.** The figure shows selection criteria and the resulting numbers of pre-selected Blazhko star candidates for each criterion and their combinations. The dots represent each case a star can occupy, where every solid dot is a specific criterion that is satisfied. Connections between solid dots represent stars which satisfy multiple criteria. Each dot combination has its own count, represented by the horizontal countplot. The vertical countplot shows the total number of stars that satisfy one criteria (union of all cases).

We used a simple scoring algorithm, optimized through trial and error, such that for LINEAR the range  $1.8 < \chi^2_{dof} < 3.0$  was worth 2 points and  $\chi^2_{dof} > 3.0$  worth 3 points, while for ZTF  $2.0 < \chi^2_{dof} < 4.0$  and  $\chi^2 > 4.0$  were the analogous limits. In addition, we also considered normalized period differences ( $dP$ ) and amplitude differences ( $dA$ ) and assigned: 2 points for  $0.00002 < dP < 0.00005$  and 4 points for  $dP > 0.00005$ ; 1 point for  $0.05 < dA < 0.15$  and 2 points for  $dA > 0.15$ . A star could score a maximum of 12 points, and a minimum of 5 points was required for further visual analysis.

The sample pre-selected using this method includes 189 stars. For most selected stars, the  $\chi^2_{dof}$  values were larger for the ZTF data because the ZTF photometric uncertainties are smaller than for the LINEAR data set. Fig. 3 summarizes the selection criteria and the resulting numbers of selected stars for each criterion and their combinations.

### 3.2. Periodogram Analysis

When light curve modulation is due to double-mode oscillation with two similar oscillation frequencies (periods), it is possible to recognize its signature in the periodogram computed as part of the Lomb-Scargle analysis. Depending on various details, such as data sampling and the exact values of periods, amplitudes, this method may be more efficient than direct light curve analysis (Skarka et al. 2020).

A sum of two *sine* functions with same amplitudes and with frequencies  $f_1$  and  $f_2$  can be rewritten using trigonometric equalities as

$$y(t) = 2 \cos(2\pi \frac{f_1 - f_2}{2} t) \sin(2\pi \frac{f_1 + f_2}{2} t). \quad (2)$$

We can define

$$f_o = \frac{f_1 + f_2}{2}, \quad (3)$$

and

$$\Delta f = \left| \frac{f_1 - f_2}{2} \right|, \quad (4)$$

with  $\Delta f \ll f_o$  when  $f_1$  and  $f_2$  are similar. The fact that  $\Delta f$  is much smaller than  $f_o$  means that the period of the *cos* term is much larger than the period of the basic oscillation ( $f_o$ ). In other words, the *cos* term acts as a slow amplitude modulation of the basic oscillation. When the amplitudes of two *sine* functions are not equal, the results are more complicated but the basic conclusion about amplitude modulation remains. When the power spectrum of  $y(t)$  is constructed, it will show 3 peaks: the main peak at  $f_o$  and two more peaks at frequencies  $f_o \pm \Delta f$ . We used this fact to construct an algorithm for automated searching for the evidence of amplitude modulation. Fig 4 compares the theoretical periodogram produced by interference beats with our algorithm's periodogram, signifying that local Blazhko peaks are present in real data.

After the strongest peak in the Lomb-Scargle periodogram is found at frequency  $f_o$ , we search for two equally distant local peaks at frequencies  $f_-$  and  $f_+$ , with  $f_- < f_o < f_+$ . The side-band peaks can be highly asymmetric Alcock et al. (2003) and observed periodograms can sometimes be much more complex Szczygieł & Fabrycky (2007). We fold the periodogram through the main peak at  $f_o$ , multiply the two branches and then search for the strongest peaks in the resulting folded periodogram that is statistically more significant than the background noise. The background noise is computed as the scatter of the folded periodogram estimated from the interquartile range. We require a “signal-to-noise” ratio of at least 5, as well as the peak strength of at least 0.05. If such a peak is found, and it doesn't correspond to yearly alias, we select the star as a candidate Blazhko star and compute its Blazhko period as

$$P_{BL} = |f_{-,+} - f_o|^{-1},$$

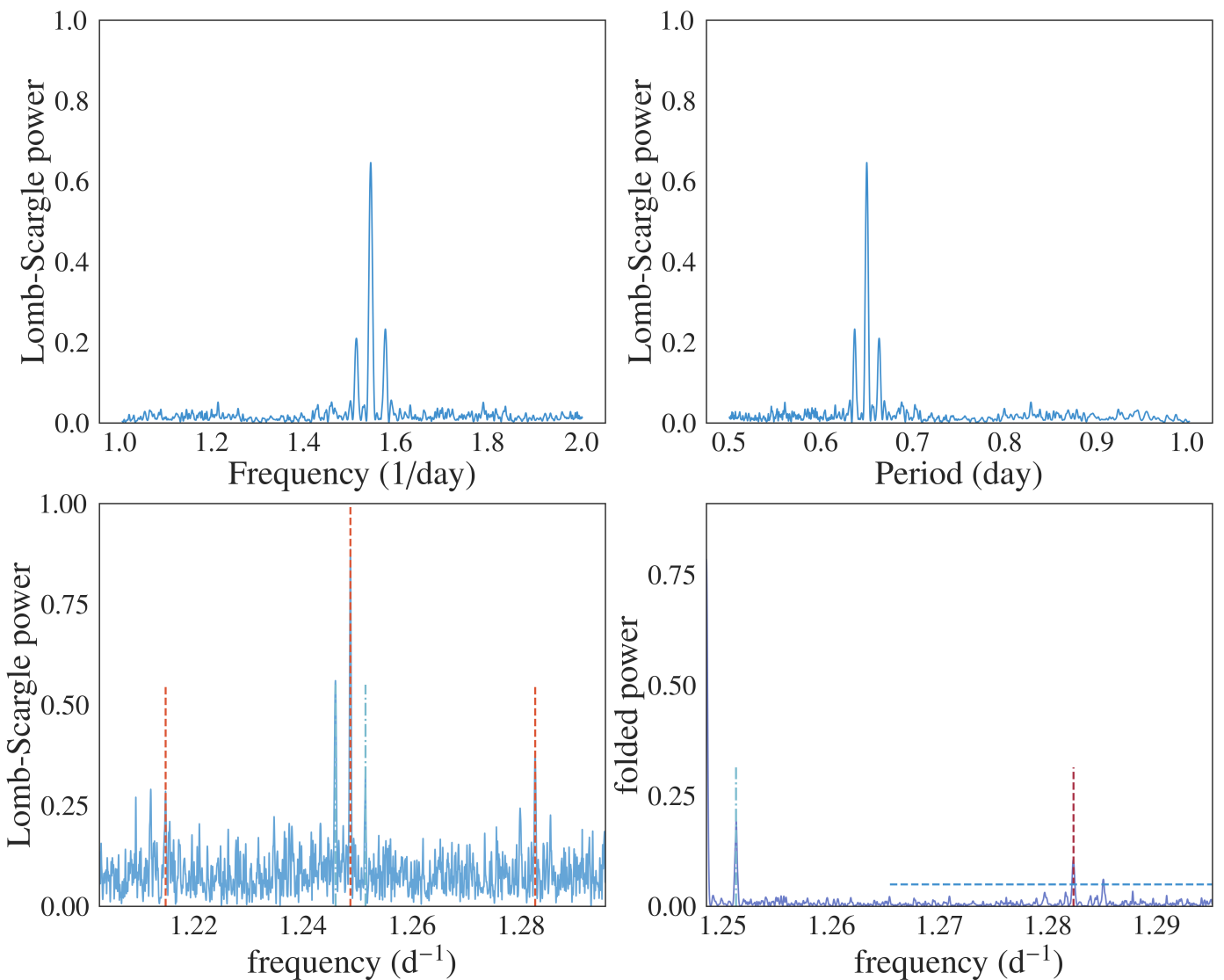


**Fig. 4.** The top two panels show a simulated periodogram for a sum of two *sine* functions with similar frequencies  $f_1$  and  $f_2$  – the central peak corresponds to their mean (see eqs. 3 and 4). The bottom left panel shows a periodogram for an observed LINEAR light curve, and the bottom right panel shows its folded version (around the main frequency  $f_o = 1.585 \text{ d}^{-1}$ ). In the bottom left panel, the three vertical dashed lines show the three frequencies identified by the algorithm described in text, and the two dot-dashed lines mark yearly aliases around the main frequency  $f_o$ , at frequencies  $f_o \pm 0.00274 \text{ d}^{-1}$ . The two vertical lines in the bottom right panel have the same meaning, and the horizontal dashed line shows the noise level multiplied by 5.

where  $f_{-,+}$  means the Blazhko sideband frequency with a higher amplitude is chosen.

The observed Blazhko periods range from 3 to 3,000 days, and Blazhko amplitudes range from 0.01 mag to about 0.3 mag (Szczygieł & Fabrycky 2007). In this work, we selected a smaller Blazhko range due to the limitations of our data: 30–325 days. With this additional constraint, we selected 51 candidate Blazhko stars, with one star already included in the sample of 189 stars described in preceding section. Fig ?? shows an example where two very prominent peaks were identified in the LINEAR periodogram.

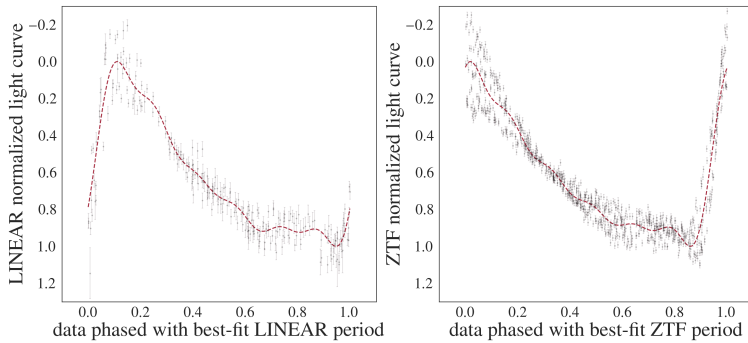
### 3.2.1. Visual Confirmation

The sample pre-selected for visual analysis includes 239 RR Lyrae stars (189 + 51, with one star selected twice), or 8.4% of the starting LINEAR-ZTF sample. Visual analysis included

the following standard steps (e.g., Jurcsik et al. 2009; Prudil & Skarka 2017):

1. The shape of the phased light curves and scatter of data points around the best-fit model were examined for signatures of anomalous behavior indicative of the Blazhko effect. Fig. 5 shows an example of such behavior where the ZTF data and fit show multiple coherent data point sequences offset from the best-fit mean model.
2. Full light curves were inspected for their repeatability between observing seasons (Fig. 6). This step was sensitive to amplitude modulations with periods of the order a year or longer.
3. The phased light curves normalized to unit amplitude were inspected for their repeatability between observing seasons. This step was sensitive to phase modulations of a few percent or larger on time scales of the order a year or longer. Fig. 7 shows an example of a Blazhko star where season-to-

STAR 160 from 239



LINEAR period chi robust: 2.1, LINEAR mean period chi robust: 2.1  
ZTF period chi robust: 4.4, ZTF mean period chi robust: 4.4  
LINEAR period chi: 8.7, LINEAR mean period chi: 8.7  
ZTF period chi: 34.2, ZTF mean period chi: 34.2  
LINEAR period: 0.545073, ZTF period: 0.545074, Period difference: 0.0  
Average LINEAR magnitude: 15.25  
LINEAR amplitude: 0.75, ZTF amplitude: 0.82

**Fig. 5.** An illustration of visual analysis of phased light curves for the selected Blazhko candidates. The left panel shows LINEAR data and the right panel shows ZTF data (symbols with “error bars”) for star with LINEARid = 1212611. The dashed lines are best-fit models. The numbers listed on the right side were added to aid visual analysis. Note multiple coherent data point sequences offset from the best-fit mean model in the right panel.

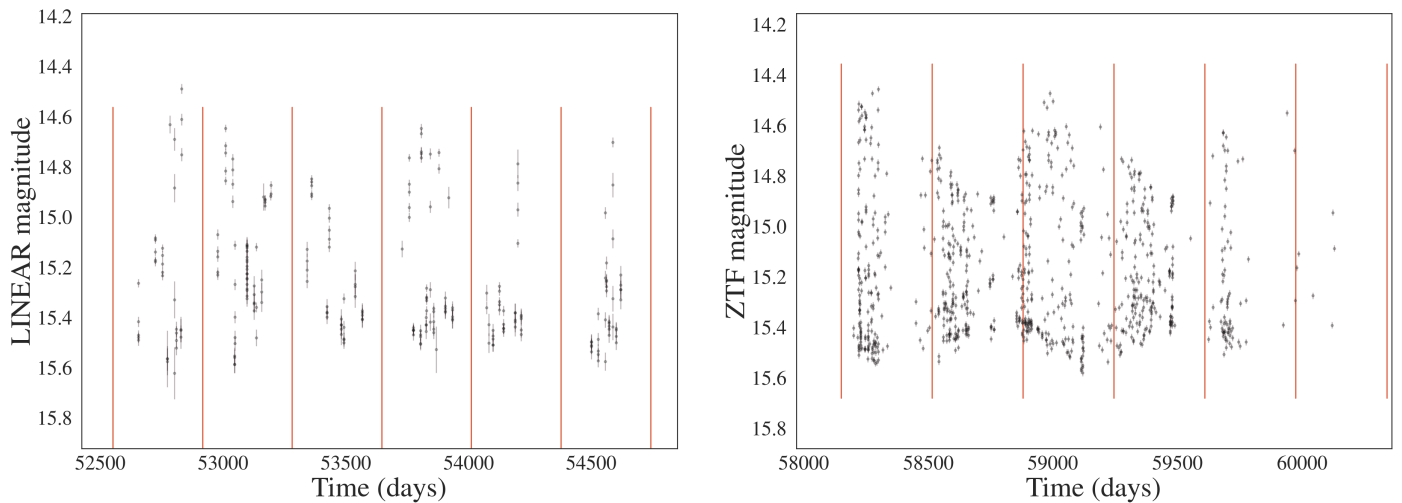


**Fig. 6.** An illustration of visual analysis of full light curves for the selected Blazhko candidates with emphasis on their repeatability between observing seasons, marked with vertical lines (left: LINEAR data; right: ZTF data). Data shown are for star with LINEARid = 1212611.

261 season phase (and amplitude) modulations are seen in both  
262 the LINEAR data and (especially) the ZTF data.

263 After visually analyzing the starting sample of 239 Blazhko  
264 candidates, we visually confirmed expected Blazhko behavior  
265 for 136 stars (112 out of 189 and 24 out of 50). LINEAR IDs  
266 and other characteristics for confirmed Blazhko stars are listed  
267 in Table 1 (Appendix A). Statistical properties of the selected  
268 sample of Blazhko stars are discussed in detail in the next section.  
269

270 STOPPED HERE

## 271 4. Results

### 272 UNFINISHED

273 Starting with a sample of 2857 field RR Lyrae stars with both  
274 LINEAR and ZTF data, we found 136 stars exhibiting convincing  
275 Blazhko effect. In Appendix A, the reader can find all of the  
276 Blazhko stars and some elementary data describing each star.

277 Another important note highlighting the difficulty of finding  
278 Blazhko stars is that the absolute Blazhko frequency difference  
279 from the main frequency is approximately  $0.028 d^{-1}$ . Also, the  
280 average period difference between LINEAR and ZTF in Blazhko  
281 stars was around 0.0001 days. These minimal differences require  
282 precise observations over a long temporal baseline.

Finally, we have discovered that in some Blazhko stars, the  
effect cannot be detected ten years later or beforehand. When  
comparing LINEAR and ZTF data, some pairs have the effect  
present in only one dataset and others in both. This finding could  
mean that the Blazhko effect is not always present and gives us a  
clue about its mechanism. However, the precision of data is also  
a factor for consideration.

## 290 5. Discussion and Conclusions

### 291 UNFINISHED

292 The reported incidence rates for the Blazhko effect range  
from 5% (Szczygieł & Fabrycky 2007) to 60% (Szabó et al.  
293 2014). For a relatively small sample of 151 stars with Kepler  
294 data, a claim has been made that essentially every RR Lyrae star  
295 exhibits modulated light curve (Kovacs 2018). The difference in  
296 Blazhko incidence rates for the two most extensive samples, ob-  
297 tained by the OGLE-III survey for the Large Magellanic Cloud  
298 (LMC, 20% out of 17,693 stars; Soszyński et al. 2009). More-  
299 over, the Galactic bulge (30% out of 11,756 stars; Soszyński  
300 et al. 2011) indicates a possible variation of the Blazhko inci-  
301 dence rate with underlying stellar population properties. In this  
302 work, 4.67% of the original RR Lyrae dataset are Blazhko stars.  
303 Since our sample size is considerable, we conclude that the in-

## Seasons for: 10030349

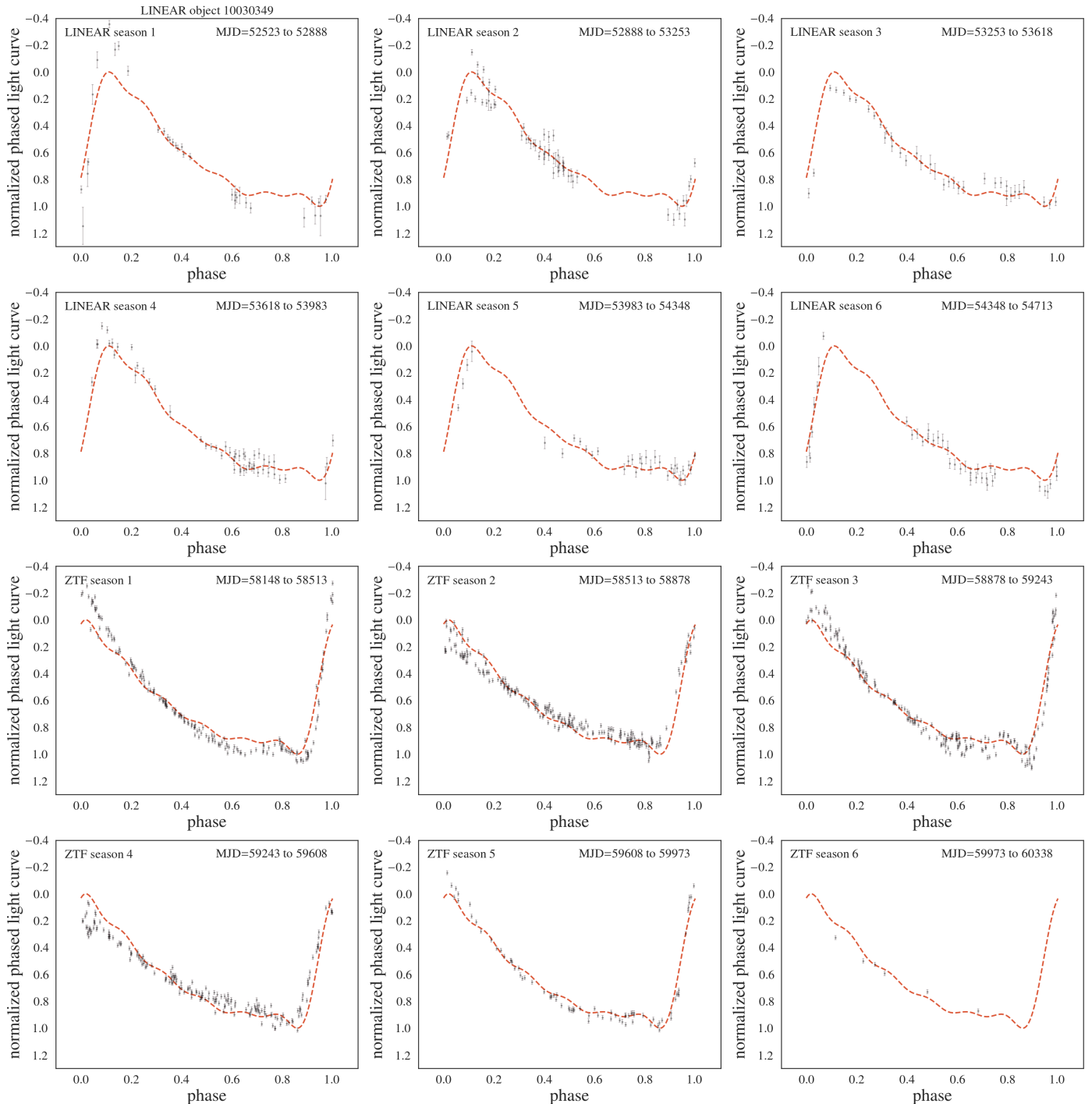


**Fig. 7.** The phased light curves normalized to unit amplitude are shown for single observing seasons and compared to the mean best-fit models (top six panels: LINEAR data; bottom six panels: ZTF data). Data shown are for star with LINEARid = 1212611. Season-to-season phase and amplitude modulations are seen in both the LINEAR and the ZTF data.

cidence rate of Blazhko stars in our work is representative and  
 305 aligns with other works. We theorize that the difference in in-  
 306 cidence rates occurs due to varying data precision, the temporal  
 307 baseline length, and differences in visual or algorithmic analysis.  
 308 We also conclude that our algorithm's success rate in finding 136  
 309 out of 239 potential Blazhko stars is 57%. This high number in-  
 310 dicates that the algorithm is very successful and can be used and  
 311 refined further for efficient Blazhko star selection.

For future research, we would like to explore the final finding  
 312 and find a connection or a factor that might give rise to a mecha-  
 313 nism that explains the Blazhko effect. The project is an excellent  
 314 example of automatizing the search for Blazhko stars. It can fur-  
 315 ther be improved by training a neural network to replace visual  
 316 analysis, and our current algorithms can be improved with other  
 317 models. This work can provide a base for finding more Blazhko  
 318 stars for the future Vera Rubin observatory. The Legacy Survey  
 319

of Space and Time (LSST; Ivezić et al. 2019) will be an excellent survey for studying Blazhko effect (Hernitschek & Stassun 2022) because it will have both a long temporal baseline (10 years) and a large number of observations per object (nominally 825; LSST Science Requirements Document<sup>4</sup>).

Claim from the abstract: With time-resolved photometry expected from LSST, a similar analysis will be performed for RR Lyrae stars in the southern sky and we anticipate a higher fraction of discovered Blazhko stars due to better sampling and superior photometric quality. Support with this quote:

the incidence rate of the Blazhko effect increases with sensitivity to small-amplitude modulation, and thus with photometric data quality (Jurcsik et al. 2009).

We confirm that the light curve modulation can be unstable, as discussed by Jurcsik et al. (2009)

(Skarka et al. 2020) classify Blazhko stars in 6 classes using the morphology of their amplitude modulation (though we note that the most dominant class includes 90% of the sample). They find bimodal distribution of Blazhko periods, with two components centered on 48 d and 186 d.

LINEAR and ZTF data used here do not have as many data points as OGLE-III used by them (comment earlier, in Introduction? also Kepler is great, (Benkő et al. 2010)). Emphasize 22 years from the start of LINEAR to the end of ZTF light curves. Also, ZTF goes deeper.

From Jurcsik et al. (2009): A sample of 30 RRab stars was extensively observed, and light-curve modulation was detected in 14 cases. The 47 per cent occurrence rate of the modulation is much larger than any previous estimate.

**Acknowledgements.** We thank Mathew Graham for providing *ztfquery* code example to us. Ž.I. acknowledges funding by the Fulbright Foundation and thanks the Ruđer Bošković Institute (Zagreb, Croatia) for hospitality. Based on observations obtained with the Samuel Oschin Telescope 48-inch and the 60-inch Telescope at the Palomar Observatory as part of the Zwicky Transient Facility project. ZTF is supported by the National Science Foundation under Grants No. AST-1440341 and AST-2034437 and a collaboration including current partners Caltech, IPAC, the Weizmann Institute of Science, the Oskar Klein Center at Stockholm University, the University of Maryland, Deutsches Elektronen-Synchrotron and Humboldt University, the TANGO Consortium of Taiwan, the University of Wisconsin at Milwaukee, Trinity College Dublin, Lawrence Livermore National Laboratories, IN2P3, University of Warwick, Ruhr University Bochum, Northwestern University and former partners the University of Washington, Los Alamos National Laboratories, and Lawrence Berkeley National Laboratories. Operations are conducted by COO, IPAC, and UW. The LINEAR program is funded by the National Aeronautics and Space Administration at MIT Lincoln Laboratory under Air Force Contract FA8721-05-C-0002. Opinions, interpretations, conclusions and recommendations are those of the authors and are not necessarily endorsed by the United States Government.

## References

|  |     |
|--|-----|
| Alcock, C., Alves, D. R., Becker, A., et al. 2003, ApJ, 598, 597   | 369 |
| Astropy Collaboration, Price-Whelan, A. M., Sipőcz, B. M., et al. 2018, AJ, 156, 123   | 370 |
| Bellm, E. C., Kulkarni, S. R., Graham, M. J., et al. 2019, PASP, 131, 018002   | 371 |
| Benkő, J. M., Kolenberg, K., Szabó, R., et al. 2010, MNRAS, 409, 1585  | 372 |
| Blažko, S. 1907, Astronomische Nachrichten, 175, 325   | 373 |
| Catelan, M. 2009, Ap&SS, 320, 261  | 374 |
| Hernitschek, N. & Stassun, K. G. 2022, ApJS, 258, 4  | 375 |
| Ivezić, Ž., Kahn, S. M., Tyson, J. A., et al. 2019, ApJ, 873, 111  | 376 |
| Jurcsik, J., Sódor, Á., Szeidl, B., et al. 2009, MNRAS, 400, 1006  | 377 |
| Kolenberg, K. 2008, in Journal of Physics Conference Series, Vol. 118, Journal of Physics Conference Series (IOP), 012060  | 378 |
| Kovács, G. 2009, in American Institute of Physics Conference Series, Vol. 1170, Stellar Pulsation: Challenges for Theory and Observation, ed. J. A. Guzik & P. A. Bradley, 261–272 | 379 |
| Kovács, G. 2016, Communications of the Konkoly Observatory Hungary, 105, 61  | 380 |
| Kovács, G. 2018, A&A, 614, L4  | 381 |
| Mizerski, T. 2003, Acta Astron., 53, 307   | 382 |
| Palaversa, L., Ivezić, Ž., Eyer, L., et al. 2013, AJ, 146, 101   | 383 |
| Prudil, Z. & Skarka, M. 2017, MNRAS, 466, 2602   | 384 |
| Sesar, B., Ivezić, Ž., Grammer, S. H., et al. 2010, ApJ, 708, 717  | 385 |
| Sesar, B., Ivezić, Ž., Stuart, J. S., et al. 2013, AJ, 146, 21   | 386 |
| Sesar, B., Stuart, J. S., Ivezić, Ž., et al. 2011, AJ, 142, 190  | 387 |
| Skarka, M., Prudil, Z., & Jurcsik, J. 2020, MNRAS, 494, 1237   | 388 |
| Smith, H. A. 1995, Cambridge Astrophysics Series, 27   | 389 |
| Soszyński, I., Dziembowski, W. A., Udalski, A., et al. 2011, Acta Astron., 61, 1   | 390 |
| Soszyński, I., Udalski, A., Szymański, M. K., et al. 2010, Acta Astron., 60, 165   | 391 |
| Soszyński, I., Udalski, A., Szymański, M. K., et al. 2009, Acta Astron., 59, 1   | 392 |
| Szabó, R. 2014, in IAU Symposium, Vol. 301, Precision Asteroseismology, ed. J. A. Guzik, W. J. Chaplin, G. Handler, & A. Pigulski, 241–248   | 393 |
| Szabó, R., Benkő, J. M., Paparó, M., et al. 2014, A&A, 570, A100   | 394 |
| Szczygiel, D. M. & Fabrycky, D. C. 2007, MNRAS, 377, 1263  | 395 |
| Vanderplas, J. 2015, gatspy: General tools for Astronomical Time Series in Python  | 396 |
| VanderPlas, J., Connolly, A. J., Ivezić, Z., & Gray, A. 2012, in Proceedings of Conference on Intelligent Data Understanding (CIDU, 47–54  | 397 |

<sup>4</sup> Available as ls.st/srd

**Appendix A: Full table of results**

407

Here we present all the confirmed Blazhko stars with their LINEAR IDs, equatorial coordinates, and calculated periods and  $\chi^2$  values.

408

409